Fairly Adjusted Multimode Dynamic Guard Bandwidth Admission Control Over CDMA Systems

Oliver Yu, *Member, IEEE*, Emir Saric, *Student Member, IEEE*, and Anfei Li

***Abstract*—Guard-based call admission control schemes support admission priorities based on resources sharing with differentiated resource capacity limits. To minimize deviation from call blocking/dropping targets due to nonstationary call arrival condition, dynamic guard-based schemes with predictive adaptation control adjust differentiated capacity limits according to predicted future arrival rates based on specified estimation algorithms. Existing dynamic guard admission schemes are developed under the assumption of perfect estimation, which may not be possible in a highly nonstationary environment and, thus resulting in failures to maintain targeted blocking/dropping probabilities. This paper presents the fairly adjusted multimode-dynamic guard bandwidth scheme, which is a dynamic-guard-based scheme over code-division multiple-access systems with predictive adaptation control to adapt interference-based guard loading-limits under nonstationary call arrival condition; and reactive adaptation control to counteract arrival rate estimation errors. When the predictive adaptation control policy mode is not able to maintain long-term call blocking or dropping targets due to estimation error, this will trigger reactive adaptation control policy modes that include temporary blocking (preemption) of one or more lower priority classes subject to fairness constraints to ensure lower priority classes are not preempted at all costs during estimation error recovery. Analytical and simulation results show that proposed scheme is able to provide performance guarantees in terms of dropping probabilities under nonstationary traffic arrival and imperfect arrival rate estimation.**

***Index Terms*—Adaptive prioritized call admission control, code-division multiple-access (CDMA)-based dynamic guard bandwidth, multitransition truncated Markov chain, reactive adaptation control.**

I. Introduction

TO ANTICIPATE the growing user demand for wireless multimedia services, future cellular wireless networks are expected to provide a diverse range of voice, video, and data services to wireless mobile users with guaranteed quality-of- service (QoS). The Universal Mobile Telecommunication System (UMTS), which is a Third-Generation (3G) Mobile Communication System developed by the European Telecommunication Standards Institute (ETSI), specifies performance guaranteed packet data services to mobile users over a wideband code-division multiple-access (WCDMA) or time-division CDMA (TD-CDMA) air-interface.

Manuscript received January 17, 2005; revised June 30, 2005. This work was supported in part by the National Science Foundation (NSF) under Grant SCI-0129527.

The authors are with the Department of Electrical and Computer Engineering, University of Illinois at Chicago, Chicago, IL 60607 USA (e-mail: oyu@ece.uic.edu; esaric2@uic.edu; ali2@uic.edu).

Digital Object Identifier 10.1109/JSAC.2005.862403

There are four QoS classes defined for UMTS network, namely, conversational, streaming, interactive, and background [1]. Each class has its own application-level QoS requirements in terms of delay, jitter, bit-error rate (BER), throughput, and burstiness, as well as call-level QoS requirements in terms of call blocking/dropping probabilities. This requires medium access control (MAC) and call admission control (CAC) protocols to, respectively, enable application-level and call-level performance guarantees for the QoS classes. This paper focuses on CAC with call-level QoS guarantees.

In a mobile wireless system, the CAC needs to differentiate admission priorities according to the call request types (handoff/new) and traffic classes. It should provide prioritized admission to handoff requests to enable lower dropping probability relative to new calls, since forced terminations of ongoing call sessions due to handoff dropping are generally more objectionable than new calls blocking from the user's perspective. In addition, handoffs of delay-stringent real-time (RT) traffic classes should have higher admission priorities relative to handoffs of nonreal-time (NRT) traffic classes.

For time-division multiple-access (TDMA) systems, the resource-sharing-based static guard channel scheme [2], [3] supports prioritized admission by assigning greater channel capacity limits to handoff requests over new calls. In [4], the dynamic guard channel scheme adapts the number of guard channels in a radio cell according to the current estimate of the handoff arrival rate derived from the current number of ongoing calls in neighboring cells and the mobility pattern, so as to keep the handoff dropping probability close to the targeted objective, while constraining the new call dropping probability to be below a given level. In [5], the dynamic guard channel scheme is extended to include multiple traffic classes; the handoff dropping probabilities are minimized at any cost without considering the degradation of the new call dropping probability. In [6], the dynamic guard channel scheme is applied in General Packet Radio Service (GPRS) systems for multiple traffic classes, while maintaining the new call dropping probability not to exceed a specified threshold.

On the other hand, QoS-enabled CAC schemes for CDMA systems have also been proposed. The capacity in CDMA systems (especially in uplink) is interference-limited, and subject to the variation of signal-to-interference ratios (SIRs), and bandwidth demands of users with limited power constraints. CDMA system loading factor can be derived to denote interference-based CDMA resources occupied by users once admitted into system. The schemes in [7] and [8] admit calls based on QoS requirements of traffic classes in terms of their interference-based loading. The schemes in

[9] and [10] support call-type and traffic-class-based admission priorities and allow prioritized traffic QoS degradation of already admitted calls to increase system capacity. The concept of guard channel-based CAC can be extended to CDMA systems through interference-limited capacity and guard loading. The static-guard-based scheme in [11], [12] and the dynamic-guard-based scheme in [13] support admission priorities based on call types and traffic classes.

Future generation wireless mobile systems will deploy more microcells and picocells to enable higher usage capacity and lower power requirements, thus increasing the frequency of handoffs and dramatizing the effects of nonstationary call arrival or loading condition. Dynamic adaptation of admission priorities to nonstationary loading can employ either predictive control ([4]–[6], [14]) based on future estimated arrival rates, or congestion-based control ([10], [15], [16]) based on current monitored call blocking/dropping probabilities. Under a highly nonstationary environment, congestion-based adaptation control schemes would incur large deviation from performance targets and low resource utilization. Similarly, performance of predictive adaptation control schemes would degrade in the presence of arrival rate estimation error inherent in a highly nonstationary environment. While performance degradation could be minimized by employing more robust and complex call arrival rate estimation algorithm (e.g., Kalman filter [14]), perfect estimation is unlikely in a highly nonstationary environment, and it is important for predictive adaptation control scheme to provide estimation error recovery. Extra resources can be preassigned to protect against underestimation error but this would lead to unnecessary resource underutilization in periods of low handoff arrivals.

To enable estimation error recovery with efficient resource utilization, this paper presents the Fairly Adjusted Multimode Dynamic Guard Bandwidth (FAM-DGB) CAC scheme. It is an extension of the Adjusted Multimode Dynamic Guard Bandwidth (AM-DGB) scheme the authors presented in [17]. FAM-DGB is a CDMA-based dynamic guard scheme with predictive adaptation control to adapt guard loading-limits under nonstationary arrival process; and reactive adaptation control to counteract arrival rate estimation errors. When the predictive adaptation control policy mode is not able to maintain long-term call blocking or dropping targets due to estimation error, this will trigger reactive adaptation control policy modes that include temporary blocking (preemption) of one or more lower priority classes. In contrast to AM-DGB [17], FAM-DGB also adds some degree of fairness constraints in the reactive adaptation control policy modes so that lower priority classes are not preempted at all costs during estimation error recovery. In addition to aforementioned contributions, this paper also presents nonstationary performance analysis of the proposed scheme via the concept of pointwise stationary approximation (PSA).

This paper is organized as follows. Section II introduces the system model, as well as formal definition of the problem statement. Then, Section III presents the proposed FAM-DGB scheme in details. Section IV presents the analysis and simulations performed under nonstationary scenario. Section V presents numerical results, and finally, Section VI concludes this work.

TABLE I
ADMISSION PRIORITY CLASSES

Admission Priority Class	UMTS Traffic Class	Call Request Type	QoS Parameter	
			R_b(kb/s)	BER
1 RT/Handoffs	Conversational and Streaming	Handoff	16	10^{-3}
2 NRT/Handoffs	Interactive and Background	Handoff	32	10^{-5}
3 RT/New	Conversational and Streaming	New Call	16	10^{-3}
4 NRT/New	Interactive and Background	New Call	32	10^{-5}

II. SYSTEM MODEL, BACKGROUND, AND PROBLEM STATEMENT

A. System Model

Admission control in a single cell of a CDMA cellular wireless system is considered. The cell consists of mobile users seeking admission (i.e., seeking access to CDMA resources) by sending admission requests to the base station (BS), which centrally implements admission algorithm and decides if a request is to be granted resources. Admission requests could originate from mobile users initiating new calls within the cell, or from mobile users who are involved in ongoing calls and entering the cell from neighboring cells. The latter requests are classified as handoff requests. In addition to being a new or handoff, call admission request can be further classified according to its traffic class requirement. This paper considers two traffic classes, namely, RT and NRT. Thus, total of four admission classes are considered, in order of descending priority: class 1 of RT handoffs, class 2 of NRT handoffs, class 3 of RT new calls, and class 4 of NRT new calls. Table I shows the performance requirements of these four admission classes. Note, however, that the proposed admission scheme concept as presented in the next section could be extended to an arbitrary number of admission classes.

It is assumed that each cell has a fixed amount of CDMA resources available, and the concept of *loading* is hereto used to denote current resource usage (i.e., CDMA "bandwidth" occupancy) as clarified next. Assume an N traffic-class system ($N = 2$; i.e., RT and NRT in this paper). Let $G_{p,k}$ be the processing gain of a user that belongs to traffic-class k ($k = 1, \ldots, N$), defined as $G_{p,k} = W/R_k$, where W is the system bandwidth in Hertz (or chip rate), and R_k is the bit rate of user of traffic class k. Assume N_k users of traffic-class k are currently in the system. Then, it can be shown (see Appendix I for complete derivation) that loading η in a CDMA system is given as

$$\eta = (1+\beta) \cdot \sum_{k=1}^{N} N_k \cdot \left[1 + \frac{G_{p,k}}{\left(\frac{E_b}{I_0}\right)_k \cdot v_k} \right]^{-1} \tag{1}$$

where $(E_b/I_0)_k$ is the signal energy per bit to noise plus interference ratio required for acceptable BER for user of traffic class k, β is the factor accounting for interference from other cells, and v_k is the activity factor of user of traffic class k. Easily measured at BS, the loading represents amount of resources used in a CDMA system, and it defines so-called "CDMA bandwidth." Note from the summation in (1) that users of different traffic classes add to loading in discrete increments $\Delta\eta_k$ (see Appendix I). These increments depend on the bit rate R_k and $(E_b/I_0)_k$ requirement of a traffic class k that user belongs to. Accordingly, and without any loss of generality, for $N = 2$ (i.e.,

$k \in \{\mathrm{RT}, \mathrm{NRT}\}$), RT and NRT connections (new calls or handoffs) are assumed to increment loading by $\Delta\eta_{\mathrm{RT}}$ and $\Delta\eta_{\mathrm{NRT}}$, respectively. Let the maximum loading supported by a cell be denoted with η_T, which is a function of the utmost interference that a cell is able to tolerate given the BER constraints and limited (mobile) transmit powers. It is also defined and completely derived mathematically in Appendix I.

B. Dynamic Guard CAC Background

Guard channel CAC schemes belong to a family of reservation-based admission schemes. They enable prioritized resource access and admission by allocating different resource capacity limits to different admission request classes. The difference in capacity limits denotes the guard channels reserved for the higher priority classes. For example, in a two-class system with C total resources, the capacity limits for the higher and lower priority classes are C and $K \leq C$, respectively. Accordingly, in this two-class system, requests from higher priority class are admitted whenever free resources are available, while requests from lower priority class are admitted only if the number of occupied resources is less than capacity-limit K. Thus, in effect, number of guard resources ($NG = C - K$) are reserved exclusively for the higher priority class. Guard schemes can be classified as either static or dynamic. Static guard schemes utilize constant capacity-limit K that is determined *a priori*, while dynamic guard schemes dynamically predictive-adapt it to maintain targeted dropping probabilities when subjected to nonstationary arrival processes. The predictive adaptation control is based on estimated future request arrival rates or some similar measure of anticipated future traffic. Some variants of dynamic guard schemes instead, employ reactive adaptation control by adapting capacity limits based on some monitored quantity such as dropping probability.

C. Problem Statement

Dynamic guard adaptation in current literature is mostly based on predictive control that relies on perfect estimation of future request arrival rates. While this might be adequate in a stationary environment, estimation errors are imminent under highly nonstationary conditions. It is a widely accepted view, however, that due to smaller cell size, traffic in the future wireless networks is expected to be highly nonstationary. Arrival rate estimation errors could significantly degrade the performance of a dynamic guard-based scheme. To demonstrate error effect further, consider three commonly used prediction methods for estimating request arrival rate $\hat{\lambda}_i[n]$ of class i at current time interval denoted by n. First method is to use the arrival rate observed at the previous time interval $n-1$ (i.e., $\hat{\lambda}_i[n] = \lambda_i[n-1]$). The second one is to use average arrival rate based on observed history (i.e., $\hat{\lambda}_i[n] = \sum_{j=1}^{n-1} \lambda_i[j]/[n-1]$). The third method is based on moving average of the first two methods. From these estimation techniques, it is evident that they are prone to errors in a highly nonstationary environment subject to sudden bursts of request arrivals. Even more sophisticated estimation techniques, such as the one based on Kalman filtering approach [14], are vulnerable in such an environment. Since capacity loading limits in a dynamic guard-based scheme are functions of these estimated request arrival rates (or of some similar traffic measure), the estimation errors will cause their erroneous computation, and this will degrade dropping probability performances as a consequence. On the other hand, dynamic guard schemes based only on reactive adaptation control try to circumvent the problem of estimation inaccuracies, by adapting capacity limits based on some monitored quantities such as dropping probabilities. Reactive adaptation control alone, however, fails to react quickly enough and is not adequate in a highly fluctuating nonstationary environment. This paper proposes dynamic guard scheme with both predictive and reactive adaptations of capacity limits to counteract arrival rate inaccuracies, while at the same time still being able to quickly react to nonstationary conditions.

III. Proposed Scheme

FAM-DGB scheme is proposed as a multiclass dynamic guard-based admission scheme suitable for CDMA systems and modified to counteract problems that arise in a highly nonstationary environment. The proposed scheme is characterized with the following features.

- It supports multiple admission priorities.
- It employs *guard loading-limits* to denote resource capacity limits. To maintain targeted dropping probabilities under nonstationary request arrival environment, the loading-limits are *predictive-adapted* based on estimation of future request arrival rates, and in order to counteract arrival rates estimation errors they are also *reactive-adapted* based on feedback information provided by current dropping probabilities.
- Under reactive control, FAM-DGB employs multiple adaptation control modes, which consist of pure dynamic guard mode (no preemption) and mixed dynamic guard and preemption modes (preempt one or more admission classes). For each admission class, *preemption thresholds* to block one, or more, lower priority admission classes are defined. If measured dropping probability of an admission class rises above a predefined preemption threshold, then reactive-adaptation control would switch into another a*daptation-control mode* that preempts one lower priority admission class. The higher the preemption threshold, the more of lower priority admission classes would be blocked if the threshold were exceeded.
- It adds a degree of fairness to the reactive adaptation control by introducing *maximum dropping thresholds* for low priority classes such that they are not preempted at all costs.

A. FAM-DGB Architecture

The architecture of FAM-DGB (shown in Fig. 1) consists of *prioritized admission controller*, and *dynamic guard adaptation controller*. Prioritized admission controller makes admission decisions based on current network load (i.e., measured η value), current guard loading-limits, and priority class of admission requests. Dynamic guard adaptation controller adapts guard loading-limits (used by admission controller) based on estimates of future arrival rates so as to keep dropping probabilities below targeted values (predictive adaptation control).

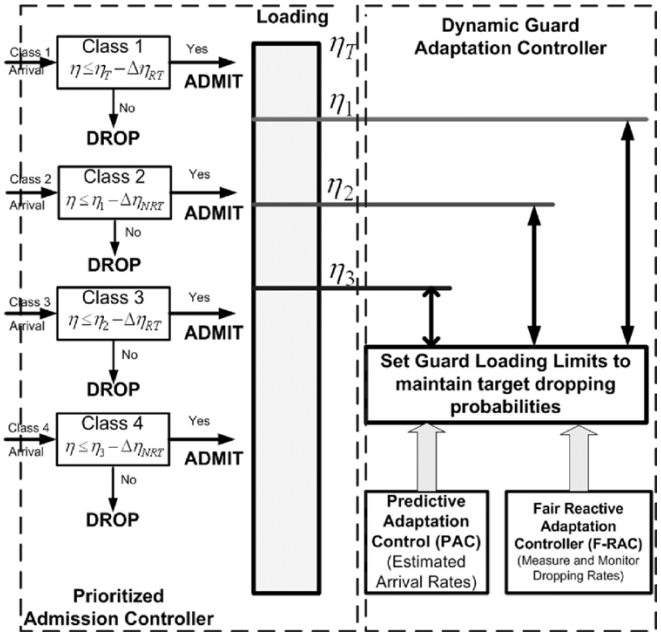

Fig. 1. FAM-DGB system.

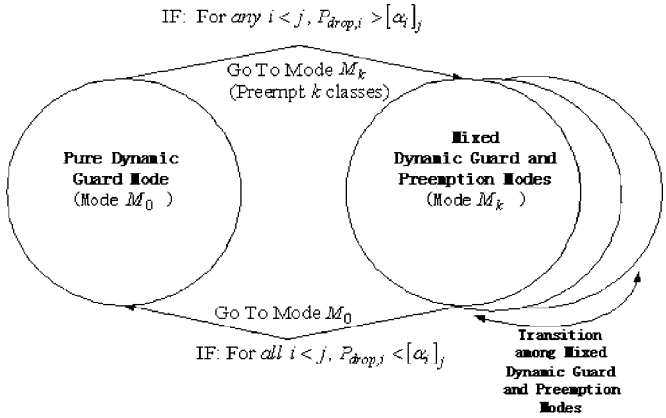

Fig. 2. Transition among adaptation modes.

It also monitors dropping probabilities in RT and makes reactive multimodal adjustment of guard loading-limits if dropping probabilities rise above preemption thresholds (reactive adaptation control) but, however, also taking into consideration maximum dropping thresholds of lower priority classes.

1) Prioritized Admission Controller: Using instantaneously measured loading η defined above [theoretically given by (1)] as the instantaneous measure of resources occupied, dynamic guard admission concept is extended to CDMA-based network by using multiple guard loading-limits. Let η_T, η_1, η_2, and η_3 be the guard loading-limits for class 1, 2, 3, and 4, respectively, where η_T is the maximum loading that can be tolerated. Then, (see left block of Fig. 1), lowest priority class 4 calls (NRT new) are admitted if and only if the current network load is less than $\eta_3 - \Delta\eta_{\rm NRT}$ (i.e., if $\eta \le \eta_3 - \Delta\eta_{\rm NRT}$). Otherwise, they are dropped. Similarly, class 3 calls (RT new) are admitted if the current network load is less than $\eta_2 - \Delta\eta_{\rm RT}$ (i.e., if $\eta \le \eta_2 - \Delta\eta_{\rm RT}$), with $\eta_2 > \eta_3$. Otherwise, they are dropped. Class 2 calls (NRT handoff) are admitted if the current network load is less than $\eta_1 - \Delta\eta_{\rm NRT}$, with $\eta_1 > \eta_2$ and, otherwise, they are dropped. The highest priority class 1 calls (RT handoff) are admitted as long as there is any free "bandwidth" to accommodate the bandwidth requirement (i.e., as long as current loading is below $\eta_T - \Delta\eta_{\rm RT}$).

2) Dynamic Guard Adaptation Controller: The dynamic guard adaptation controller consists of predictive and fair-reactive adaptation controllers.

a) Predictive Adaptation Controller (PAC): For a four-class system, PAC dynamically adapts the guard loading-limits η_j ($j = 1,2,3$) of class $j+1$ based on the analytical model developed in Section III that relates estimated arrival rates and dropping probabilities (see right block of Fig. 1). For given estimated arrival rates (of all classes), loading-limits η_j's are set in every time interval n such as to maintain dropping probabilities of all classes below their respective targeted values. The targeted value of a class is its lowest preemption threshold. Estimated arrival rates depend on the current number of ongoing calls in neighboring cells, as well as on the mobility model. The actual arrival rates estimation method is not discussed in this paper, but a reader can refer to [4] and [14] for examples.

b) Fair–Reactive Adaptation Controller (F-RAC): For presentation clarity, we first explain unfair-RAC operation (as in [17]), and then at the end of this subsection elaborate further on the fairness extension. For an N-admission priority classes system, N adaptation control modes $(M_0, M_1, \ldots, M_{N-1})$ would be specified. M_0 is a pure dynamic guard mode without any class preemption, while all M_k (for $k \neq 0$) are mixed dynamic guard and preemption modes with k lower priority admission classes being preempted by forcing corresponding guard loading-limits to zero. Fig. 2 shows transitions from M_0 (pure dynamic guard mode) to $M_1, \ldots, M_{N-1}$ (mixed dynamic guard and preemption modes), and among themselves. RAC selects adaptation control modes based on current measured dropping probabilities of the admission classes and class-dependent predefined preemption thresholds. Dropping probability of class i or $P_{{\rm drop},i}$ is given as the ratio of class i dropped calls to total class i admission requests. If $P_{{\rm drop},i}$ is greater than a predefined preemption threshold $[\alpha_i]_j$ of class i, then all lower priority classes starting from j are to be preempted or blocked by setting corresponding guard loading-limits to zero. Except for the lowest admission class that could not specify preemption threshold, class i specifies from 1 to $(N-i)$ preemption thresholds. The lowest preemption threshold of each class is set equal to the target dropping probability of that class.

Fig. 3 illustrates the preemption thresholds and adaptation control modes for a four-class system. Class 4 requests ($j = 4$) are preempted (i.e., guard loading-limit η_3 is set to zero) if $P_{{\rm drop},i}$ of any of the higher priority classes $i < j$ ($i = 1,2,3$) exceeds its *dropping target* or the lowest preemption threshold $[\alpha_i]_4$ (i.e., $P_{\rm drop1} > [\alpha_1]_4$ or $P_{\rm drop2} > [\alpha_2]_4$, or $P_{\rm drop3} > [\alpha_3]_4$); and the RAC would switch the adaptation control mode to M_1, where guard loading-limit of class 4 (η_3) is set to zero, while other loading-limits are still predictive-adapted by PAC. Requests of classes 3 and 4 are preempted (i.e., guard loading-limits η_2 and η_3 are set to zero) if $P_{\rm drop1} > [\alpha_1]_3$ or $P_{\rm drop2} > [\alpha_2]_3$, and the RAC would switch to adaptation control mode M_2 where the loading-limit

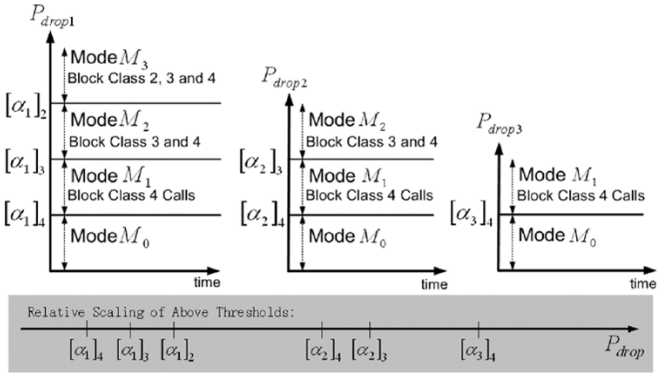

Fig. 3. Preemption thresholds and multiple modes used by dynamic adaptation controller in a four-class system.

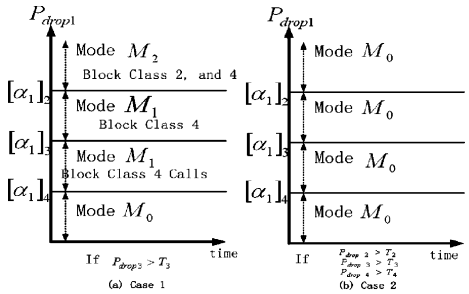

Fig. 4. Example of adaptation control modes used by FAM-DGB scheme.

η_1 is still predictive-adapted by PAC. Similarly, requests of classes 2, 3, and 4 are preempted (i.e., guard loading-limits η_1, η_2 and η_3 are set to zero) if $P_{\text{drop1}} > [\alpha_1]_2$, and the RAC would switch to adaptation control mode M_3, where only class 1 is allowed admission.

Unfair-RAC, however, preempts lower priority classes at all costs whenever monitored dropping probability of higher priority classes is above corresponding preemption thresholds. This may lead to high dropping degradations of lower priority classes in the event of high loading, as investigated in [17]. In order to account for this and make the admission scheme fair to lower priority classes, F-RAC defines *maximum dropping thresholds* T_j for class j, (j = 2,3,4). If monitored dropping probability of class j, is above its corresponding maximum dropping threshold (i.e., if $P_{\text{drop},j} > T_j$), that particular class is not preemptied even if dropping probability of any of higher priority class i ($i < j$) exceeds its dropping target $[\alpha_i]_j$. The class j, instead, continues to operate in pure dynamic guard mode M_0 where its corresponding guard loading-limit η_{j-1} is predictive-adapted by PAC.

To illustrate the concept by an example, Fig. 4 shows adaptation control modes used by F-RAC of FAM-DGB for two example cases; Case 1: dropping probability of class 3 only exceeds its maximum dropping threshold, $P_{\text{drop},3} > T_3$; $P_{\text{drop},2} < T_2$; $P_{\text{drop},4} < T_4$ [see Fig. 4(a)]; and Case 2: dropping probability of lower priority classes 2, 3, and 4 exceeds their respective maximum dropping thresholds, $P_{\text{drop},2} > T_2$; $P_{\text{drop},3} > T_3$; $P_{\text{drop},4} > T_4$ [see Fig. 4(b)]. As can be seen in Fig. 4(a) for Case 1, even if $P_{\text{drop},1}$ would exceed $[\alpha_1]_3$ [or if $P_{\text{drop},2}$ would exceed $[\alpha_2]_3$, not shown in Fig. 4(a)], F-RAC would not preempt class 3 because $P_{\text{drop},3} > T_3$. It would instead remain in adaptation control mode M_1 with only class 4 preempted as $P_{\text{drop},4} < T_4$. On the other hand, for Case 2 [Fig. 4(b)], F-RAC would remain in adaptation control mode M_0 (no preemptions) regardless of current dropping values of higher priority classes (Fig. 4 shows example for $P_{\text{drop},1}$). Therefore, as evident from the above example, in effect, lower priority classes are not preempted at all costs by FAM-DGB.

c) Initial Tuning of F-RAC System Parameters: The operating system parameters (i.e., preemption thresholds $[\alpha_i]_j$ and maximum dropping thresholds T_j) are network operator specific constants. Their initial tuning depends on operator's level of class dependent QoS provisioning. In this section, probabilistic tuning is suggested as follows. It is assumed that operator has long-term measurements of call arrivals and dropping rates available for each class, and that based on these averages it is able to distribute resources fairly such as to (probabilistically) guarantee QoS level of each class in terms of its long-term dropping probability. Consequently, operator defines dropping target for each class i such that the probability (or percentage of time) its observed dropping rate $P_{\text{drop},i}$ exceeds dropping target is less than some provisioned QoS-level, denoted as δ_i. In an N-class system, the lowest preemption threshold $[\alpha_i]_N$, of each class i (except the lowest priority one) is set to this dropping target. Mathematically, therefore, $\text{P}\{P_{\text{drop},i} > [\alpha_i]_N\} \leq \delta_i$. In order to guard against future nonstationary arrivals, other preemption thresholds for class i, (i.e., $[\alpha_i]_j$ for $j < N$) are set similarly. Mathematically, they are also determined from long-term measured data, such that following relation is satisfied: $\text{P}\{P_{\text{drop},i} > [\alpha_i]_j\} \leq \delta_{i,j}$, with $\delta_{i,j} > \delta_i$.

On the other hand, maximum dropping threshold T_j, for class j (except for class 1) is defined as the "soft" dropping target that is to be maintained when a system operates under high congestion. For class j, thus, T_j is set to its maximum-tolerable dropping rate. In accordance with the above tuning suggestion, the ordering of system parameters in an N-class system is, thus, $[\alpha_i]_N < [\alpha_i]_{N-1} < \cdots < [\alpha_i]_{i+1} < T_i$.

IV. Performance Analysis and Simulation Model

FAM-DGB scheme is analyzed in a *nonstationary* environment. Simulation model utilizing an event-driven simulator OPNET [22], [23] is also presented. Four admission classes defined previously are considered. Performance measures are dropping probabilities. Also, an analytical model used by PAC of FAM-DGB admission scheme is developed.

A. Stationary Markov Model and PAC Procedure (Four-Class System)

1) General Markov Model: Let the arrivals of class 1, 2, 3, and 4 calls be governed by four independent (stationary) Poisson processes each with mean arrival rate of λ_1, λ_2, λ_3, and λ_4 (calls/s), respectively. Also, define cumulative mean arrival rates of RT (handoffs and new calls) and NRT (handoffs and new calls) traffic classes as $\lambda_{\text{rt}} = \lambda_1 + \lambda_3$ and $\lambda_{\text{nrt}} = \lambda_2 + \lambda_4$, respectively. Moreover, assume that the time a connection of class i holds resources in a cell is exponentially distributed random variable with mean $1/\mu_i$ seconds. In order to obtain tractable solution and without any loss of generality, it is assumed in the analysis model that the overall resource holding time is exponentially distributed with mean $1/\mu$ which is given as the average of all individual $1/\mu_i$ quantities. In the simulation model

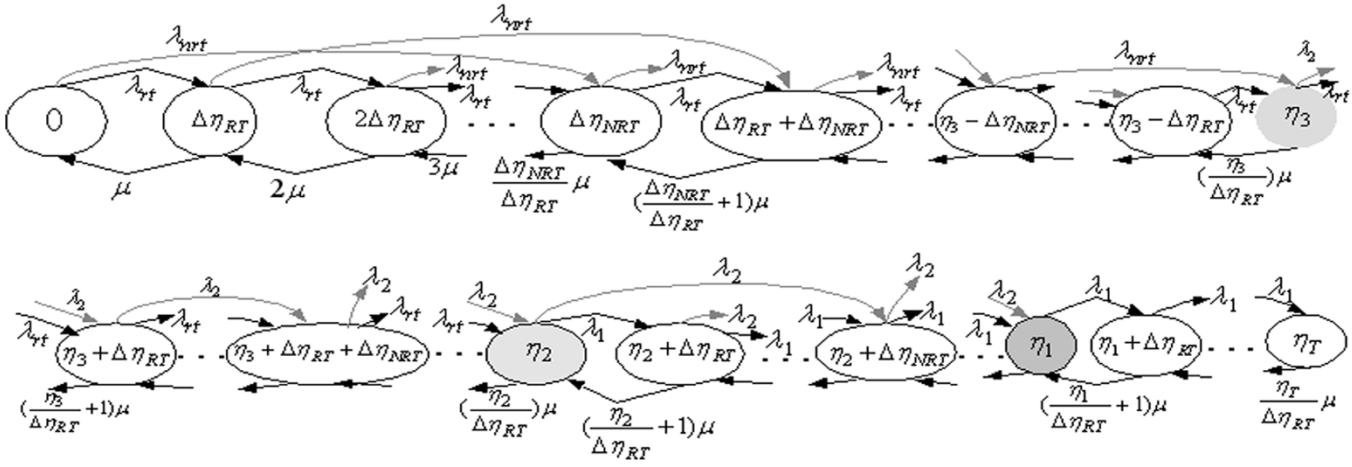

Fig. 5. Multitransition truncated $M/M/\eta_T/\eta_T$ loss mode.

(as presented later), the first simulation scenario models different holding times per class i with means $1/\mu_i$, and the second simulation scenario models the overall average single holding time with mean $1/\mu$ as in analysis.

Let the state of the system be current loading η (i.e., amount of resources occupied). As explained earlier, loading (i.e., state) is incremented discretely, such that an admitted connection of a RT traffic class (1 and 3) and NRT traffic class (2 and 4) increases loading η by $\Delta\eta_{\mathrm{RT}}$ and $\Delta\eta_{\mathrm{NRT}}$, respectively. Without any loss of generality, let $\Delta\eta_{\mathrm{NRT}} = k \cdot \Delta\eta_{\mathrm{RT}}$ for some integer k. Then, operation of the proposed scheme (with PAC) can be modeled as a *multitransition truncated* $M/M/\eta_T/\eta_T$ loss system with state-dependent arrival rates as depicted by Markov chain diagram in the Fig. 5. "Multitransition" means that from a given state η, transition could lead to states $\eta+\Delta\eta_{\mathrm{RT}}$ and $\eta+\Delta\eta_{\mathrm{NRT}}$, with different transition rates depending on the traffic class of admitted connection. Meanwhile, "truncated" means that arrival rates change (i.e., they are "truncated") when the current loading reaches the state given by guard loading limits η_i (see Fig. 5). From transition rates given in Fig. 5, the generator (or transition rate) matrix $\mathbf{Q} = [q_{ij}]$ can be obtained, as shown in (2) at the bottom of the page.

The nondiagonal entries of matrix $\mathbf{Q}$ (i.e., $q_{ij}\ \forall i \neq j$) are the rates at which the process moves from state i to state j. On the other hand, the diagonal entries of $\mathbf{Q}$ (i.e., q_{ii}) are obtained by subtracting the rate at which process departs state i from 1 (i.e., $q_{ii} = 1 - \sum_{i=0, i\neq j}^{\eta_T} q_{ij}$). This definition implies that the rows of $\mathbf{Q}$ sum to 1. Furthermore, it also implies that 1 is always an eigenvalue of $\mathbf{Q}^T$ (where T denotes vector or matrix transpose operation). Therefore, for the system in Fig. 5, q_{ij} entries of the generator matrix are given, as shown in (3-a)–(3-e) at the bottom of the next page.

From Fig. 5, it is evident that all states of a chain communicate (as there is a path that connects them) in nonperiodic manner. Consequently, this Markov chain is irreducible and, thus, the steady-state probabilities exist and they satisfy balancing equations. Let the steady-state probability of state j ($j = 0, \Delta\eta_{\mathrm{RT}} \ldots \eta_T$) be denoted as P_j. Also, define a column vector P that contains all steady-state probabilities (i.e., $\mathrm{P}^T = [P_0, P_{\Delta\eta_{\mathrm{RT}}}, \ldots, P_{\eta_T}]$). Then, using Markov chain theory, global balance (or equilibrium) equations can be expressed in matrix form as

$$\mathbf{Q}^T\mathrm{P} = \mathrm{P}. \tag{4}$$

The normalization condition is

$$1^T\mathrm{P} = 1 \tag{5}$$

where 1^T is the all-unity vector $[1, \ldots, 1]$. The equilibrium equation implies that P is the eigenvector of $\mathbf{Q}^T$ with corresponding eigenvalue of 1. Let $\mathrm{V}_k = [v_{k,i}]$ denote the eigenvector of $\mathbf{Q}^T$ with corresponding eigenvalue k. The steady-state probabilities of above model are, thus, given as (after proper normalization)

$$\mathrm{P} = \frac{\mathrm{V}_1}{(\Sigma v_{1,i})}. \tag{6}$$

Dropping probabilities are then obtained by summing over these probabilities (see Fig. 5)

$$P_{\mathrm{drop1}} = P_{\eta_T},\ \ P_{\mathrm{drop2}} = \sum_{j=\eta_1}^{\eta_T} P_j$$
$$P_{\mathrm{drop3}} = \sum_{j=\eta_2}^{\eta_T} P_j,\ \ P_{\mathrm{drop4}} = \sum_{\eta_3}^{\eta_T} P_j. \tag{7}$$

$$\mathbf{Q} = \begin{bmatrix} q_{00} & q_{0\Delta\eta_{\mathrm{RT}}} & q_{0\Delta\eta_{\mathrm{NRT}}} & \cdots & q_{0\eta_T} \\ q_{\Delta\eta_{\mathrm{RT}}0} & q_{\Delta\eta_{\mathrm{RT}}\Delta\eta_{\mathrm{RT}}} & q_{\Delta\eta_{\mathrm{RT}}\Delta\eta_{\mathrm{NRT}}} & \cdots & q_{\Delta\eta_{\mathrm{RT}}\eta_T} \\ q_{\Delta\eta_{\mathrm{NRT}}0} & q_{\Delta\eta_{\mathrm{NRT}}\Delta\eta_{\mathrm{RT}}} & q_{\Delta\eta_{\mathrm{NRT}}\Delta\eta_{\mathrm{NRT}}} & \cdots & q_{\Delta\eta_{\mathrm{NRT}}\eta_T} \\ \cdots & \cdots & \cdots & \cdots & \cdots \\ q_{\eta_T 0} & q_{\eta_T\Delta\eta_{\mathrm{RT}}} & q_{\eta_T\Delta\eta_{\mathrm{NRT}}} & \cdots & q_{\eta_T\eta_T} \end{bmatrix} \tag{2}$$

d) Simplified Truncated Loss Model: Even though the above model is tractable, the complexity of the eigenvalue problem grows as the number of states in the model increases (i.e., as size of the matrix $\mathbf{Q}$ increases). Thus, the closed-form solution for steady-state probabilities is not easily obtainable. In order to reduce computational complexity, an approximation of the above model is presented for which closed-form solution is easily obtainable. Let $\bar{\Delta}\eta$ denote the *average* loading (i.e., resource) requirement (increment) of RT and NRT connections. Using the same notation as before, it is defined as

$$\bar{\Delta}\eta = \frac{\lambda_{rt}}{\lambda_{rt}+\lambda_{nrt}} \cdot \Delta\eta_{\mathrm{RT}} + \frac{\lambda_{nrt}}{\lambda_{rt}+\lambda_{nrt}} \cdot \Delta\eta_{\mathrm{NRT}}. \quad (8)$$

Define $\lambda_{1-2} = \lambda_1 + \lambda_2$, $\lambda_{1-3} = \lambda_1 + \lambda_2 + \lambda_3$, and $\lambda_{1-4} = \lambda_1+\lambda_2+\lambda_3+\lambda_4$. By using average loading increment $\bar{\Delta}\eta$, operation of the proposed scheme can be modeled as a (birth–death) *truncated* $M/M/\eta_T/\eta_T$ loss system with state-dependent arrival rates as depicted by Markov chain diagram in the Fig. 6.

Define *normalized loading* $\varpi = \eta/\bar{\Delta}\eta$. Note that ϖ is an integer. By the same token, let *normalized loading limit* for class i (i = 2,3,4) be $\varpi_{i-1} = \eta_{i-1}/\bar{\Delta}\eta$, and let *normalized maximum loading* be $\varpi_T = \eta_T/\bar{\Delta}\eta$. For more elegant notational purposes, let state $\varpi \cdot \bar{\Delta}\eta$ (in Fig. 6) be denoted by integer ϖ. From Fig. 6, the steady-state probabilities could be obtained in closed-forms by utilizing local balancing principle. They are given in (9) at the bottom of the next page (see Appendix II for a complete derivation) where P_0 is easily obtained from the normalizing equation. Dropping probabilities are then obtained in the similar way as in (7) in the last section.

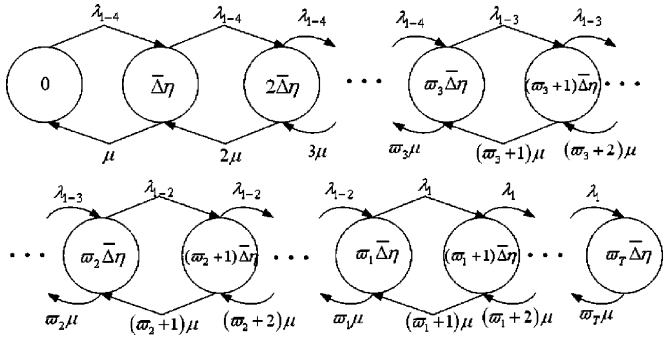

Fig. 6. Simplified truncated $M/M/\eta_T/\eta_T$ loss model.

The simplified model is validated by comparing dropping probabilities to those of the general Markov model. From numerical results presented in Fig. 7, it can be seen that dropping probabilities obtained from simplified (birth–death) truncated loss model are always close to the ones obtained from the general Markov model when class 1 arrival rate λ_1 is varied from 0 to 0.35. The results are shown for two different class 2 arrival rate values (i.e., $\lambda_2 = 0.05$ and $\lambda_2 = 0.15$), while λ_3 and λ_4 are assumed fixed at 0.05. Therefore, simplified model is a good approximation that reduces complexity by avoiding eigenvalue

$$q_{i,j} = \begin{cases} \lambda_{rt}, & \ldots j = i + \Delta\eta_{\mathrm{RT}} \\ \lambda_{nrt}, & \ldots j = i + \Delta\eta_{\mathrm{NRT}} (\forall j \le \eta_3) \\ \lambda_2, & \ldots j = i + \Delta\eta_{\mathrm{NRT}} (\forall j > \eta_3) \\ \left(\frac{i}{\Delta\eta_{\mathrm{RT}}}\right)\cdot\mu, & \ldots j = i - \Delta\eta_{RT} \\ 1 - \lambda_{rt} - \lambda_{nrt} - \left(\frac{i}{\Delta\eta_{\mathrm{RT}}}\right)\cdot\mu, & \ldots j = i \\ 0, & \ldots \text{otherwise} \end{cases} \quad \forall i < \eta_3, \quad (3\text{-a})$$

$$q_{i,j} = \begin{cases} \lambda_{rt}, & \ldots j = i + \Delta\eta_{\mathrm{RT}} \\ \lambda_2, & \ldots j = i + \Delta\eta_{\mathrm{NRT}} \\ \left(\frac{i}{\Delta\eta_{\mathrm{RT}}}\right)\cdot\mu, & \ldots j = i - \Delta\eta_{\mathrm{RT}} \\ 1 - \lambda_{rt} - \lambda_2 - \left(\frac{i}{\Delta\eta_{\mathrm{RT}}}\right)\cdot\mu, & \ldots j = i \\ 0, & \ldots \text{otherwise} \end{cases} \quad \text{for } \eta_3 \le i < \eta_2 \quad (3\text{-b})$$

$$q_{i,j} = \begin{cases} \lambda_1, & \ldots j = i + \Delta\eta_{\mathrm{RT}} \\ \lambda_2, & \ldots j = i + \Delta\eta_{\mathrm{NRT}} (\forall j \le \eta_1) \\ \left(\frac{i}{\Delta\eta_{\mathrm{RT}}}\right)\cdot\mu, & \ldots j = i - \Delta\eta_{\mathrm{RT}} \\ 1 - \lambda_1 - \lambda_2 - \left(\frac{i}{\Delta\eta_{\mathrm{RT}}}\right)\cdot\mu, & \ldots j = i \\ 0, & \ldots \text{otherwise} \end{cases} \quad \text{for } \eta_2 \le i < \eta_1 \quad (3\text{-c})$$

$$q_{i,j} = \begin{cases} \lambda_1, & \ldots j = i + \Delta\eta_{\mathrm{RT}} \\ \left(\frac{i}{\Delta\eta_{\mathrm{RT}}}\right)\cdot\mu, & \ldots j = i - \Delta\eta_{\mathrm{RT}} \\ 1 - \lambda_1 - \left(\frac{i}{\Delta\eta_{\mathrm{RT}}}\right)\cdot\mu, & \ldots j = i \\ 0, & \ldots \text{otherwise} \end{cases} \quad \text{for } \eta_1 \le i < \eta_T \quad (3\text{-d})$$

$$q_{\eta_T,j} = \begin{cases} \left(\frac{\eta_T}{\Delta\eta_{\mathrm{RT}}}\right)\cdot\mu, & \ldots j = \eta_T - \Delta\eta_{\mathrm{RT}} \\ 1 - \left(\frac{\eta_T}{\Delta\eta_{\mathrm{RT}}}\right)\cdot\mu, & \ldots j = \eta_T \\ 0, & \ldots \text{otherwise} \end{cases} \quad (3\text{-e})$$

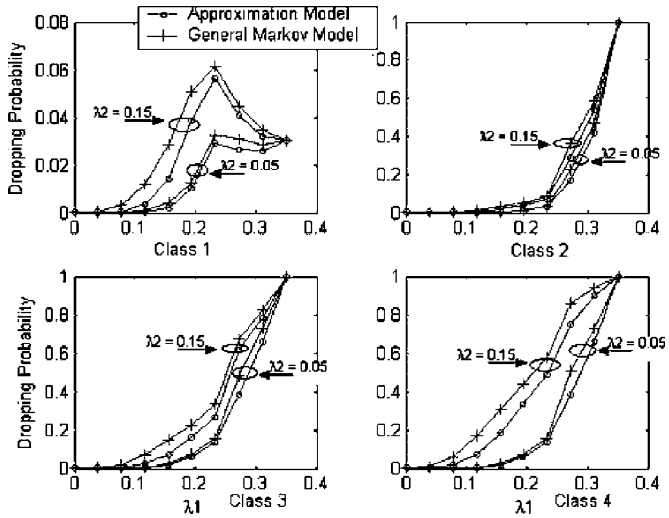

Fig. 7. Simplified model versus general Markov model.

problem, while giving closed-form solutions that will be useful during system designs.

2) PAC Loading Limit Adaptation Procedure: As mentioned in previous section guard loading-limits η_i, $i = 1, 2, 3$ are adapted dynamically by PAC. The adaptations are based on estimated arrival rates. From the above dropping (7) with P_j's from (6) or (9), maximum possible guard loading-limits η_i, $i = 1, 2, 3$ can be found for given four-tuple of arrival rates $[\lambda_1, \lambda_2, \lambda_3, \lambda_4]$, such that $P_{\text{drop1}} < [\alpha_1]_4$, $P_{\text{drop2}} < [\alpha_2]_4$ and $P_{\text{drop3}} < [\alpha_3]_4$ are all satisfied (where dropping targets (lowest preemption thresholds) $[\alpha_i]_4$ $i = 1,2,3$ are defined in last section). Accordingly, PAC of dynamic guard adaptation controller uses this mapping to dynamically set loading-limits η_i, $i = 1, 2, 3$ for given four-tuple $[\hat{\lambda}_1, \hat{\lambda}_2, \hat{\lambda}_3, \hat{\lambda}_4]$, where $\hat{\lambda}_i$ represents *estimated* arrival rate of class i. These mappings can be computed once and stored in a memory lookup table at BS.

However, assume that arrival rate estimation errors are made in dynamic guard scheme (M_0). Let arrival rate estimation error be denoted as ε. Then, the estimated arrival rate is given as $\hat{\lambda}_i = \lambda_i + \varepsilon$. With such an error, PAC from time to time *underestimates* (for negative ε) or *overestimates* (for positive ε) loading-limits needed (i.e., $\eta_i(\lambda_1, \lambda_2, \lambda_3, \lambda_4)$) to keep dropping probabilities below targets.

B. Nonstationary Analytical Model (Four-Class System)

A realistic *nonstationary* arrival model is developed in this section and is applied to the general (stationary) Markov model developed in the last subsection via pointwise-stationary approximation (PSA). In order to model such an environment, nonstationary arrivals from two handoff classes (i.e., class 1 and 2) are assumed. Without any loss of generality, it is assumed that new calls within a cell (classes 3 and 4) can still be modeled by stationary arrivals. Time is divided into equal length intervals, each of duration Δt (seconds). In each interval n ($n = 1, 2, 3, \ldots$), arrival rate $\lambda_i(n \cdot \Delta t) \equiv \lambda_i[n]$, for classes $i = 1$ and 2 is equally likely to take any value in the range [0, 0.35]. It then retains this value for the whole interval (i.e., Δt seconds).

In such an environment, FAM-DGB scheme can be analyzed using $M(t)/M/\eta_T/\eta_T$ model, where $M(t)$ stands for a nonstationary Poisson arrival process with time-dependent arrival rate function $\lambda(t)$. $M(t)/M/\eta_T/\eta_T$ systems have been analyzed extensively in the literature [18]–[21]. One very simple and good approximation is called PSA [18], [19]. According to this approximation, in each time interval, $M(t)/M/\eta_T/\eta_T$ system is analyzed in the same way as corresponding stationary $M/M/\eta_T/\eta_T$ system, with $\lambda(t)$ representing "stationary" arrival rate for the interval beginning at time instant t and lasting Δt seconds. Thus, in each time interval a stationary process is considered. For PSA estimate to be valid, a time interval Δt should be 4–5 times longer than mean resource holding time $1/\mu$.

Consequently, truncated $M/M/\eta_T/\eta_T$ model in Fig. 6 is used in this paper to get PSA estimate at each interval n (alternatively, model in Fig. 5 could also be used). Using PSA estimate, and the same notations as in the last subsection, time-dependent state probabilities $P_j(n \cdot \Delta t) = P_j[n]$ for a system with normalized guard loading-limits ϖ_1, ϖ_2, ϖ_3 (where $\varpi_i = \eta_i/\bar{\Delta}\eta$), can be obtained from Fig. 6, and shown in (10) at the bottom of the page, where $\lambda_i[n]$ now denotes *time-dependent* arrival rate of class i at the nth interval as defined before. Let

$$P(\varpi = j) = P_j = \begin{cases} \frac{\lambda_{1-4}^{j}}{j!\cdot\mu^j} \cdot P_0, & j = 1, 2, \ldots, \varpi_3 \\ \frac{\lambda_{1-4}^{\varpi_3} \cdot \lambda_{1-3}^{(j-\varpi_3)}}{j!\cdot\mu^j} \cdot P_0, & j = \varpi_3 + 1, \varpi_3 + 2, \ldots, \varpi_2 \\ \frac{\lambda_{1-4}^{\varpi_3} \cdot \lambda_{1-3}^{(\varpi_2-\varpi_3)} \cdot \lambda_{1-2}^{(j-\varpi_2)}}{j!\cdot\mu^j} \cdot P_0, & j = \varpi_2 + 1, \ldots, \varpi_1 \\ \frac{\lambda_{1-4}^{\varpi_3} \cdot \lambda_{1-3}^{(\varpi_2-\varpi_3)} \cdot \lambda_{1-2}^{(\varpi_1-\varpi_2)} \cdot \lambda_1^{(j-\varpi_1)}}{j!\cdot\mu^j} \cdot P_0, & j = \varpi_1 + 1, \ldots, \varpi_T \end{cases} \tag{9}$$

$$P_j[n] = \begin{cases} \frac{\lambda_{1-4}[n]^j}{j!\cdot\mu^j} \cdot P_0[n], & j = 1, 2, \ldots, \varpi_3 \\ \frac{\lambda_{1-4}[n]^{\varpi_3} \cdot \lambda_{1-3}[n]^{(j-\varpi_3)}}{j!\cdot\mu^j} \cdot P_0[n], & j = \varpi_3 + 1, \ldots, \varpi_2 \\ \frac{\lambda_{1-4}[n]^{\varpi_3} \cdot \lambda_{1-3}[n]^{(\varpi_2-\varpi_3)} \cdot \lambda_{1-2}[n]^{(j-\varpi_2)}}{j!\cdot\mu^j} \cdot P_0[n], & j = \varpi_2 + 1, \ldots, \varpi_1 \\ \frac{\lambda_{1-4}[n]^{\varpi_3} \lambda_{1-3}[n]^{(\varpi_2-\varpi_3)} \lambda_{1-2}[n]^{(\varpi_1-\varpi_2)} \lambda_1[n]^{(j-\varpi_1)}}{j!\cdot\mu^j} \cdot P_0[n], & j = \varpi_1 + 1, \ldots, \varpi_T \end{cases} \tag{10}$$

$\lambda_{1-2}[n] = \lambda_1[n] + \lambda_2[n]$, $\lambda_{1-3}[n] = \lambda_1[n] + \lambda_2[n] + \lambda_3[n]$, and $\lambda_{1-4}[n] = \lambda_1[n] + \lambda_2[n] + \lambda_3[n] + \lambda_4[n]$. Note that in accordance with the proposed scheme corresponding guard loading-limit is set to zero by F-RAC if a class is blocked (preempted) in that time interval. Then, the *instantaneous* PSA estimated dropping probabilities (at the nth interval), $P_{\mathrm{drop},i}(n \cdot \Delta t) = P_{\mathrm{drop},i}[n]$ are

$$P_{\mathrm{drop},1}[n] = P_{\varpi_T}[n], \quad P_{\mathrm{drop},2}[n] = \sum_{j=\varpi_1}^{\varpi_T} P_j[n],$$
$$P_{\mathrm{drop},3}[n] = \sum_{j=\varpi_2}^{\varpi_T} P_j[n], \quad P_{\mathrm{drop},4}[n] = \sum_{j=\varpi_3}^{\varpi_T} P_j[n]. \quad (11)$$

Consequently, at each time interval of duration Δt, instantaneous values of dropping probabilities are obtained with respect to the *current adaptation control mode*, current loading-limits and using (10) and (11). The adaptation control mode in turn depends on preemption threshold $[\alpha_i]_j$ values used and on the *running average* of dropping probability calculated for class i at nth time interval as

$$\overline{P}_{\mathrm{drop},i}[n] = \frac{\overline{P}_{\mathrm{drop},i}[n-1] + P_{\mathrm{drop},i}[n]}{n} \quad (12)$$

where $P_{\mathrm{drop},i}[n]$ is the *instantaneous* dropping of class i at that time interval as defined in (11). In accordance with FAM-DGB scheme, if last interval's running average $\overline{P}_{\mathrm{drop},i}[n-1]$ for class i is above corresponding preemption threshold $[\alpha_i]_j$, then lower priority classes $j > i$ for which $\overline{P}_{\mathrm{drop},j}[n-1] \leq T_j$ are blocked (i.e., corresponding guard loading-limits are set to 0) in that time interval.

C. Simulation Model

Simulation model under nonstationary environment is developed using an event-driven simulator OPNET [22], [23]. A target cell is modeled consisting of mobiles (handoff and new) seeking admission and a BS where admission algorithm is implemented. All parameters are set in accordance with the analytical model including nonstationary Poisson arrival process generated in the same fashion as in the analysis model. However, two simulation scenarios are developed depending on the modeling of random variables denoting resource holding times. The first simulation scenario models distinct resource holding times for different classes, with class i resource-holding time assumed to be exponentially distributed with mean $1/\mu_i$. On the other hand, to validate single holding time assumption used in the analytical model (when the variation of individual mean holding times is reasonably low) the second simulation scenario models single overall resource holding time with mean $1/\mu$ which is given as the average of all individual $1/\mu_i$ quantities used in the first scenario. The arrival rate estimation error ε is used as a simulation parameter in both scenarios.

V. Numerical Analysis and Simulation Results

Four guard-based schemes, proposed FAM-DGB, AM-DGB [17], Dynamic Guard and Static Guard are compared in terms of their performances in maintaining targeted dropping probabilities for different admission priority classes. Performance under perfect and imperfect arrival rate estimation conditions is investigated. Under nonstationary environment, performances are compared over a 24-hour interval using PSA analysis with time-varying arrival rates, as well as OPNET simulation. Numerical values of the general system parameters applicable to the four guard-based schemes are shown in Tables II and III. Dynamic Guard scheme is the scheme without F-RAC and adaptation control modes (i.e., it is always in mode M_0) and can be considered as a special emulation of the scheme in [13]. Unlike the other three schemes that employ dynamic adaptive capacity loading limits, Static Guard employs constant capacity loading-limits that are specified as $\eta_1 = 4\%$, $\eta_2 = 8\%$, and $\eta_3 = 12\%$ of the total bandwidth. This scheme can be considered as special case of scheme in [12].

TABLE II
General System Parameters for Analysis and Simulation

Parameter	Value
Class1 Arrival Process	Poisson in each interval with time varying mean $\lambda_1(t)$
Class2 Arrival Process	Poisson in each interval with time varying mean $\lambda_2(t)$
Class 3 Arrival Process	Poisson with mean arrival rate $\lambda_3 = 0.05$
Class 4 Arrival Process	Poisson with mean arrival rate $\lambda_4 = 0.05$
Class 1 Dropping Target	0.002
Class 2 Dropping Target	0.03
Class 3 Dropping Target	0.035
Class 4 Dropping Target	0.04
Resource Holding Time (Simulation-Scenario 1)	Exponential for each class with means (in seconds): $1/\mu_1 = 120$, $1/\mu_2 = 180$, $1/\mu_3 = 120$, $1/\mu_4 = 180$
Resource Holding Time (Analysis and Simulation-Scenario 2)	Exponential, with mean $1/\mu = \frac{1}{4}\sum_{i=1}^{4} 1/\mu_i = 150$ seconds
System Bandwidth W	1.25MHz
Activity Factor ν_k	ν_k lies between 0 and 1. 3/8 for RT traffic, 1 for NRT traffic
Out-of cell Interference Factor β	0.55

TABLE III
FAM-DGB Operational Parameters

Class 1 Preemption Thresholds	$[\alpha_1]_4 = 0.002$, $[\alpha_1]_3 = 0.0025$, $[\alpha_1]_2 = 0.003$
Class 2 Preemption Thresholds	$[\alpha_2]_4 = 0.03$, $[\alpha_2]_3 = 0.032$
Class 3 Preemption Thresholds	$[\alpha_3]_4 = 0.035$
Class 4 Preemption Thresholds	Not Applicable
Class i Maximum Dropping Threshold T_i	$T_2 = 0.036$, $T_3 = 0.038$, $T_4 = 0.045$

A. No Arrival Rate Estimation Error

Perfect estimation of arrival rates is assumed in each time interval (i.e., $\varepsilon = 0$). Under nonstationary environment, running-average of dropping probability $\overline{P}_{\mathrm{drop},i}[n]$ for class i (1–4), is shown, respectively, in Fig. 8(a)–(d) for all four schemes (analysis). Compared against the Static Guard scheme, the adaptation-based schemes (FAM-DGB, AM-DGB, and Dynamic Guard) maintain dropping probabilities of classes 1, 2, and 3 below or close to the targeted objective, but only slightly degrade dropping probability of class 4. The reason is that they adapt to nonstationary loading. Static Guard scheme on the other hand wastes resources by reserving too much guard during low arrival rates and not reserving enough during high arrival rates and is, thus, not suitable for a nonstationary environment.

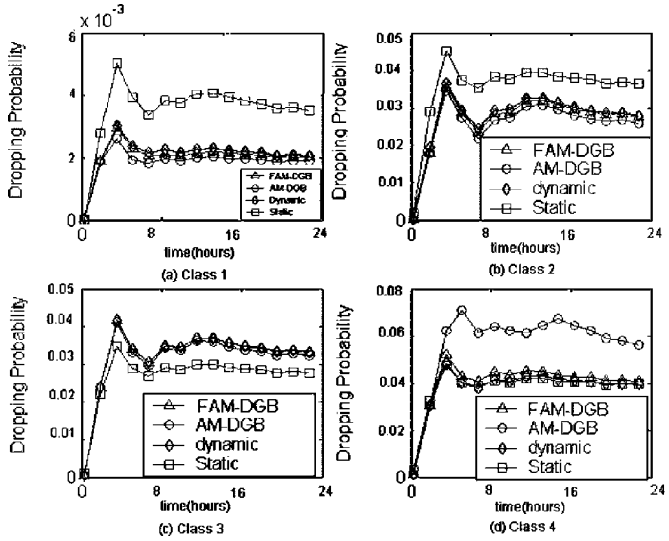

Fig. 8. Analysis: Class 1–4 dropping probability—Nonstationary (no estimation error $\varepsilon = 0$).

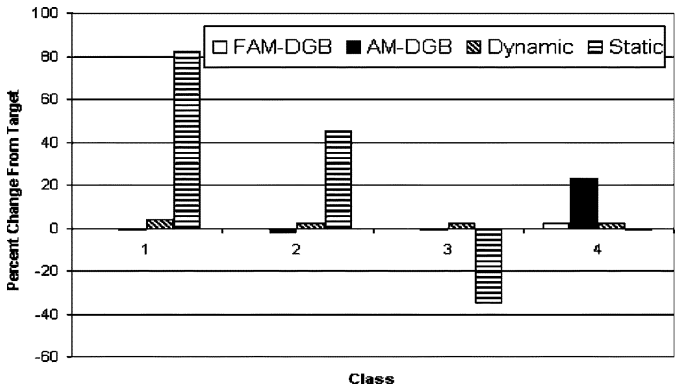

Fig. 9. Analysis: Average dropping probability change relative to targets—Nonstationary.

As can be seen in Fig. 8, AM-DGB scheme enables lower dropping probability than that of Dynamic Guard, with the exception of class 4. The reason is that AM-DGB employs additional reactive adaptation control to counteract periods of extremely high loadings. FAM-DGB scheme further accounts for degradations of lower priority classes [namely, class 4, Fig. 8(d)] by employing maximum dropping thresholds. By doing this fair adjustment, FAM-DGB only slightly degrades higher priority classes (class 1) as evident in Fig. 8(a).

Performance gain/loss is quantified in Fig. 9, which shows the percentage of deviation of the average dropping probability from the target of each class. For efficient resource utilization, ideally all dropping probabilities should be as close to target as possible. Negligible deviation means targeted objective is met, while high negative and positive deviations indicate performance gain and loss, respectively. For example, proposed FAM-DGB incurs performance gains of 1% in classes 1, 2, and 3, respectively, but performance loss of 3% in class 4. AM-DGB incurs larger performance gains of 2%, 3%, and 2% in classes 1, 2, and 3, respectively, but also large performance loss of 25% in class 4.

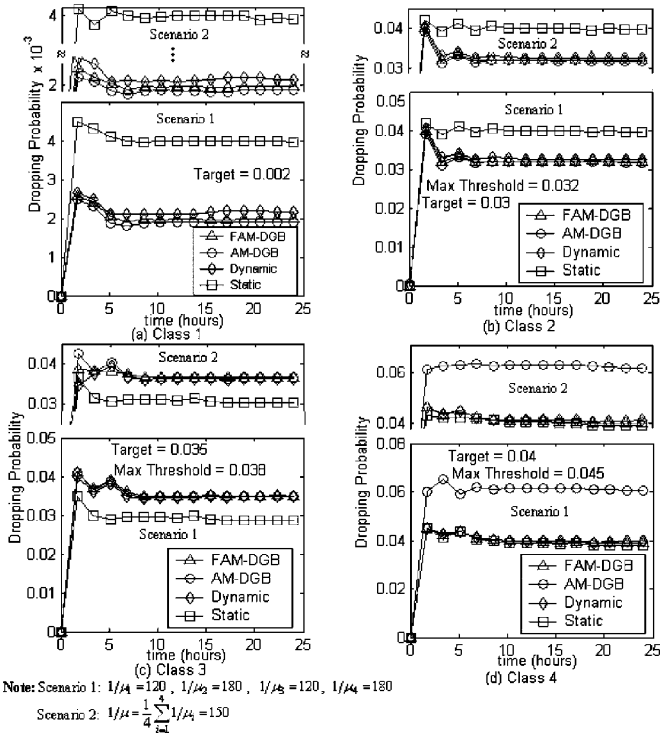

Fig. 10. Simulation: Class 1–4 dropping probability—Nonstationary (no estimation error $\varepsilon = 0$).

Let G_i and L_i denote the *relative performance gain and loss* in class i when *compared* between two schemes. Comparing FAM-DGB to AM-DGB, relative losses in classes 1, 2, and 3 are observed from Fig. 9 to be $L_1 = 1.01$ (1%), $L_2 = 1.02$ (2%), and $L_3 = 1.01$ (1%), respectively. Similarly, relative gain observed in class 4 is given by $G_4 = 1.22$ (22%). Defining the overall performance gain/loss ratio across all classes as $R = \prod G_i / \prod L_i$. Then, $R > 1$ means that overall performance gain compensates more than that of overall performance loss. For example, comparing FAM-DGB to AM-DGB, Dynamic Guard and Static Guard, R is 1.17, 1.69, and 1.94, respectively.

Corresponding OPNET simulation results (i.e., dropping probabilities) of two simulation scenarios obtained for class i (1–4) (no estimation errors) are shown in Fig. 10(a)–(d), respectively. Results of the first scenario (single overall average resource-holding time) and second scenario (distinct resource-holding times) are shown in Fig. 10. Note that the results obtained for both scenarios are in close agreement which shows that analytical assumption (single average resource-holding time) is valid when the variations of individual mean holding times is low as is assumed in this paper. Also, the results converge to the corresponding analytical results (in Fig. 8). Fig. 11 (simulation counterpart of Fig. 9) shows that the proposed FAM-DGB, as well as AM-DGB outperforms Dynamic and Static Guard schemes for first three classes. Comparing as before FAM-DGB to AM-DGB, Dynamic Guard and Static Guard, the overall gain/loss ratio defined earlier R is 1.16, 1.18, and 2.50, respectively. It is also worth mentioning that analysis and simulation results in Figs. 8 and 10, respectively, show that the system stabilizes relatively quickly (at about the eighth simulation hour).

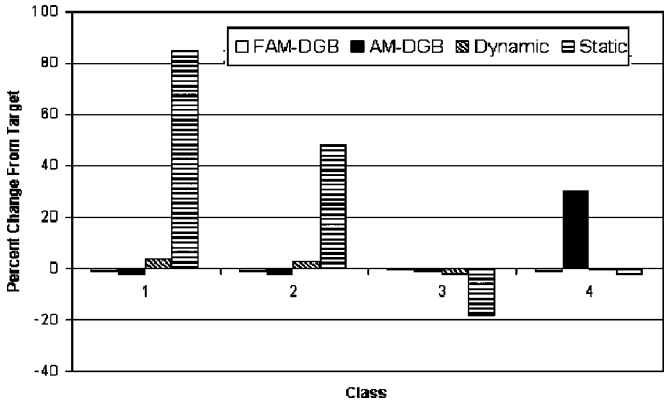

Fig. 11. Simulation: Mean dropping change relative to targeted objectives—Nonstationary.

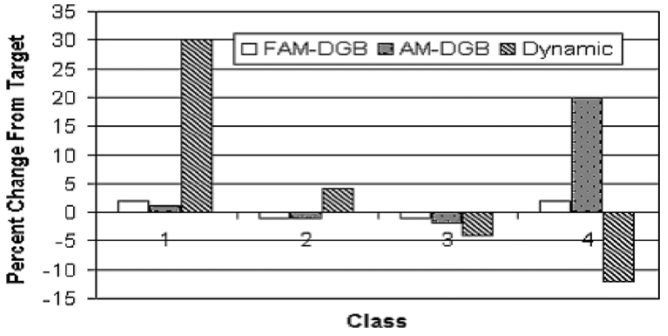

Fig. 13. Simulation: Mean dropping change relative to targeted objectives—Underestimation.

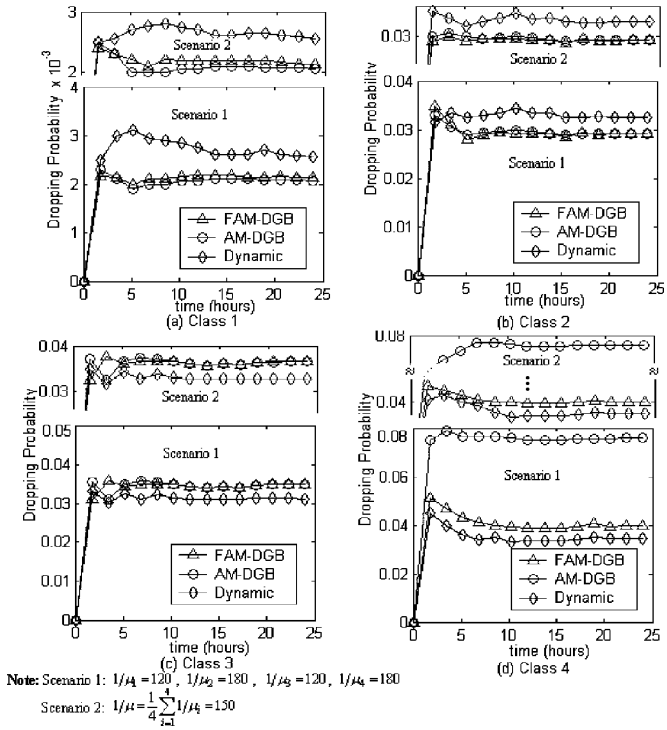

Fig. 12. Simulation: Effect of underestimation error ($\varepsilon = -0.02$).

B. Results Under Arrival Rate Estimation Error

OPNET simulation is employed to adaptive guard schemes in nonstationary environment with imperfect arrival rate estimation. Note that static guard scheme is not considered, as it is insensitive on estimated arrival rates. Estimated arrival rate is modeled as $\hat{\lambda}_i(n\Delta t) = \lambda_i(n\Delta t) + \varepsilon$, where $\lambda_i(n\Delta t)$ is the *actual* arrival rate of class i for the nth time interval and ε is the error introduced by the estimator. Dropping probabilities are evaluated for two cases, namely, underestimation (negative ε), and overestimation (positive ε).

1) Arrival Rate Underestimation Error: Underestimation of class 1 arrival rate is assumed in each time instant with error ε fixed at -0.02. Using OPNET, dropping probabilities are obtained for class i (1–4) of adaptive guard schemes (FAM-DGB, AM-DGB, and Dynamic Guard). The simulation results of two scenarios are shown in Fig. 12(a)–(d) for classes 1–4, respectively. Compared with perfect estimation case, most deviations are observed in highest and lowest priority classes (class 1 and 4). As expected, estimation error degrades performance of dynamic guard scheme by causing erroneous computation of guard-loading limits. As evident from Fig. 12(a) and as a result of arrival rate underestimation, dynamic guard scheme does not reserve enough guard for class 1. This causes its dropping probability to considerably deviate from target of 0.2%. Note from Fig. 12(d) that resources not reserved for class 1 by dynamic guard scheme are utilized by lower priority classes as evident by unintended decrease of class 4 dropping probability. By employing adaptation control modes, AM-DGB scheme on the other hand, mitigates for error effect in class 1 [see Fig. 12(a)]. However, AM-DGB does this at the expense of high dropping of lower priority classes (namely, class 4) whenever class 1 dropping is above preemption threshold. FAM-DGB accounts for this unfairness by defining maximum dropping thresholds for lower priority classes. From Fig. 12(d), it can be seen that FAM-DGB keeps class 4 at desirable level, while only slightly degrading class 1 as compared with AM-DGB scheme. Thus, it in effect "filters out" error effect and keeps dropping probabilities close to targets. This is evident in Fig. 13 which shows mean dropping deviations (both positive and negative) from targeted values where as before, the objective is to be as close to the target as possible. The results of the two simulation scenarios in Fig. 12 are in close agreements. Comparing proposed FAM-DGB to AM-DGB and to Dynamic Guard scheme, the overall relative gain/loss ratio R (defined in the last section) is 1.18 and 1.45, respectively, from Fig. 13.

2) Arrival Rate Overestimation Error: Overestimation of class 1 arrival rate is assumed in each time instant with error ε fixed at $+0.02$. The OPNET simulation results (two scenarios) for class i (1–4) shown in Fig. 14(a)–(d), respectively, and Fig. 15 are almost symmetrical to underestimation case. As expected, dynamic guard scheme is the most affected. Due to overestimation of class 1 arrival rate, the amount of guard reserved for class 1 by pure dynamic guard scheme is overestimated and its dropping probability is unintentionally decreased from target. This leads to resource underutilizations, which is evident by increase in dropping of lower priority classes. AM-DGB is the most ineffective in overestimation case as evident by high dropping of class 4 from Fig. 14(d). The reason for this is that class 4 is again preempted at all costs at time instants whenever classes 2 or 3 are above their preemption thresholds (not class 1 which has excess resources

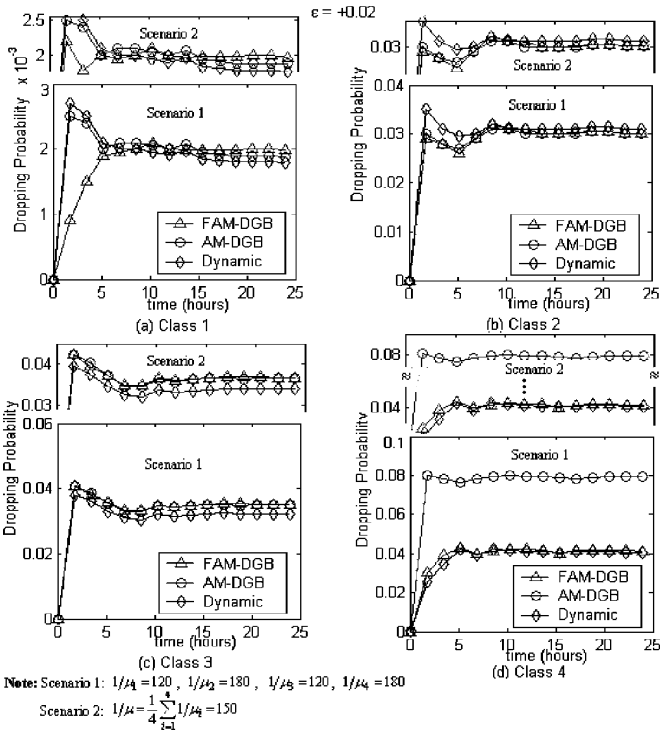

Fig. 14. Simulation: Effect of overestimation error ($\varepsilon = +0.02$).

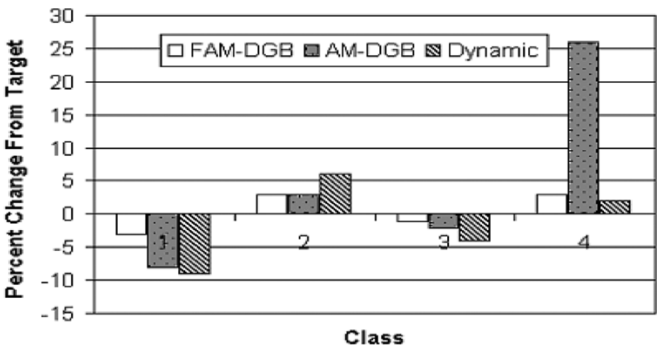

Fig. 15. Simulation: Mean dropping change relative to targeted objectives—Overestimation.

and is always below target). The degradation observed in class 4 from Fig. 15 by AM-DGB scheme is 26%. Using maximum dropping thresholds FAM-DGB mitigates for this and reduces it to 3% (see Fig. 15), while still meeting targeted objective for class 1. The results obtained for both scenarios in Fig. 14 are in close agreement.

3) Overall Relative Gain/Loss Ratio: Fig. 16 shows the overall relative gain/loss ratio R observed against absolute value of error ε. Note that according to definition, $R > 1$ means that the overall performance gain compensates more than that of overall performance loss. It can be seen that the proposed scheme outperforms the Dynamic Guard scheme by 18%–85% and the AM-DGB scheme by 16%–20%, respectively, when underestimation error ranges from 0 to 0.1 requests/s. It also can be seen that the proposed scheme outperforms the Dynamic Guard scheme by 18%–50% and the AM-DGB scheme from 16% to 27%, respectively, when overestimation error ranges from 0 to 0.1 requests/s. The Dynamic Guard scheme incurs

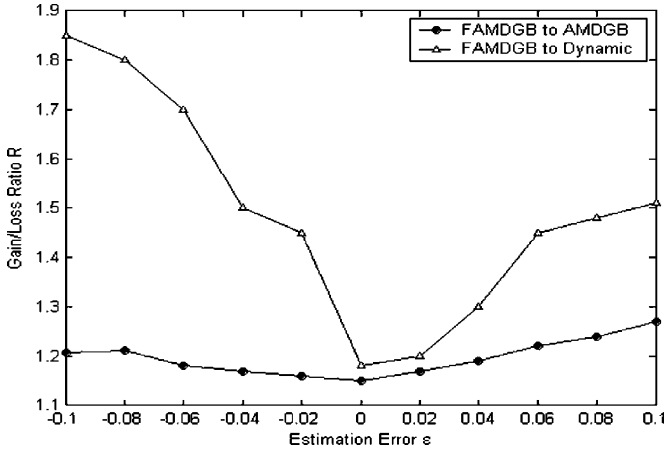

Fig. 16. Relative gain/loss ratio versus error.

the highest degradation due to the lack of an estimation error recovery mechanism. While both AM-DGB and FAM-DGB schemes employ estimation error recovery mechanism, the performance gain of the proposed FAM-DGB scheme is due to the fairness constraints that prevent overpreemption of lower priority classes at all costs.

VI. Conclusion

Proposed FAM-DGB admission scheme enables adaptive prioritized admission control in CDMA systems by extending dynamic guard concept. The proposed scheme employs both predictive and fairly adjusted reactive adaptation controls of the resource loading limits under nonstationary arrival environment. When predictive-adaptation control fails to maintain targeted dropping probabilities for higher priority admission classes, fair-reactive-adaptation control would preempt or block one or more lower priority admission classes until the failure condition ceases to exist. Preemption of lower priority classes is not performed at all costs. Performance of the proposed admission scheme is evaluated analytically and by simulations under nonstationary arrival environment. Both analytical and simulation results show that under highly variable loading, and in the presence of arrival rate estimation errors, FAM-DGB is able to maintain targeted dropping probabilities.

Appendix I
Loading Capacity in CDMA System

Assume an N-class system. The signal energy per bit to noise plus interference ratio $(E_b/I_0)_k$ of a user of class k, $k = 1, 2, \ldots, N$ (observed at BS) is given as

$$\left(\frac{E_b}{I_0}\right)_k = Gp, k \cdot \frac{S_k}{I_{\text{total}} - S_k}$$

where S_k is the received signal power of a user of class k, and I_{total} is the total received wideband power including thermal noise power P_N in the BS (processing gain $G_{p,k}$ is defined earlier in the text). Assume perfect power control such that the received power levels S_k of all users belonging to the same class k are equal. Let γ_k be the minimum $(E_b/I_0)_k$ value required for

acceptable BER (for a user of class k). Therefore, the following constraints need to be satisfied ($\forall k$):

$$\left(\frac{E_b}{I_0}\right)_k = Gp,k \cdot \frac{S_k}{I_{\text{total}} - S_k} \geq \gamma_k. \tag{13}$$

It can be shown that the received power levels are minimized when the above equation is satisfied with equality. Let S_k^* be the received power level of a user of class k such that the above equation is satisfied with equality. Thus

$$S_k^* = \frac{1}{1 + \frac{Gp,k}{\gamma_k}} \cdot I_{\text{total}}.$$

Note, however, that the received power level S_k is bounded by the maximum value $S_{k,\max}$ which is dependent on (mobile) transmit power, and achieving feasible $S_k^* \leq S_{k,\max}$ is a requirement that limits maximum interference I_{total} that a system is able to tolerate, as elaborated later. Let the load factor increment $\Delta\eta_k$ of a user of class k be defined as $\Delta\eta_k = S_k^*/I_{\text{total}}$. Therefore

$$\Delta\eta_k = \frac{1}{1 + \frac{G_{p,k}}{\gamma_k}}. \tag{14}$$

Assuming N_k users of class k are in the system, I_{total} is

$$I_{\text{total}} = \sum_{k=1}^{N} N_k \cdot S_k^* + P_N. \tag{15}$$

Let noise rise (NR) be defined as the ratio of total received wideband noise power in BS to the thermal noise power ($\text{NR} = I_{\text{total}}/P_N$). Substituting into above formulas

$$\text{NR} = \frac{I_{\text{total}}}{P_N} = \left[1 - \sum_{k=1}^{N} N_k \cdot \Delta\eta_k\right]^{-1} = \frac{1}{1-\eta}$$

where η ($\eta \geq 0$) is defined as the loading

$$\eta = \sum_{k=1}^{N} N_k \cdot \Delta\eta_k = 1 - \left(\frac{P_N}{I_{\text{total}}}\right) \leq \eta_T. \tag{16}$$

Note that after accounting for out of cell interference β, and activity factor v_k, the loading η is expressed as in (1).

A. Maximum Loading

Maximum loading, denoted as η_T, is limited by the utmost interference a system is able to tolerate (given BER and limited power $S_{k,\max}$ constraints). From (15) and (16), the total interference I_{total} can be expressed in terms of loading as $I_{\text{total}} = P_N/(1-\eta)$. Then, BER constraints become

$$G_{p,k} \cdot \frac{S_{k,\max}}{\left[\frac{P_N}{(1-\eta)}\right] - S_{k,\max}} \geq \gamma_k, \quad \forall k.$$

Equivalently, in terms of loading η

$$\eta \leq \left(1 - \frac{P_N}{\frac{(G_{p,k} \cdot S_{k,\max})}{\gamma_k} + S_{k,\max}}\right) < 1, \quad \forall k.$$

Therefore, loading bound, or the maximum loading η_T tolerated by a system is given as

$$\eta_T = \min_{\forall k}\left[1 - \frac{P_N}{\frac{(G_{p,k} \cdot S_{k,\max})}{\gamma_k} + S_{k,\max}}\right]. \tag{17}$$

APPENDIX II
DERIVATION OF STATE PROBABILITIES

Assume that a system is in *equilibrium* (i.e., it has been running for a long time). In order to obtain state probabilities one can make use of *local balance equations*. Imagine that a vertical boundary between each adjacent pair of states is drawn in Fig. 6, such that a state transition diagram is separated into two parts. Local balancing principle states that flow of *probability flux* along transition from left to right across such boundary is equal to the flow of probability flux from right to left [24]. For the state $j \cdot \overline{\Delta}\eta$, the probability flux along a transition, numerically, is the product of the state probability (P_j) at which a transition originates and the transition rate associated with transition. Therefore, looking at Fig. 6, local balance equations are

$$\lambda_{1-4} \cdot P_0 = \mu \cdot P_1 \rightarrow \therefore P_1 = \frac{\lambda_{1-4}}{\mu} \cdot P_0$$

$$\lambda_{1-4} \cdot P_1 = 2\mu \cdot P_2 \rightarrow \therefore P_2 = \frac{\lambda_{1-4}}{2\mu} \cdot P_1 = \frac{(\lambda_{1-4})^2}{2\mu^2} \cdot P_0.$$

Continuing in the same way for any $0 < j \leq \varpi_3$, we obtain

$$P_j = \frac{(\lambda_{1-4})^j}{j! \cdot \mu^j} \cdot P_0 \quad j = 1, 2, \ldots, \varpi_3. \tag{18}$$

Similarly, for $\varpi_3 < j \leq \varpi_2$, local balance equations are

$$\lambda_{1-3} \cdot P_{\varpi_3} = (\varpi_3 + 1)\mu \cdot P_{\varpi_3+1} \rightarrow \therefore P_{\varpi_3+1} = \frac{\lambda_{1-3}}{(\varpi_3+1)\mu} \cdot P_{\varpi_3} = \frac{\lambda_{1-4}^{\varpi_3} \cdot \lambda_{1-3}}{(\varpi_3+1)!\mu^{(\varpi_3+1)}} \cdot P_0 \ldots$$

Therefore

$$P_j = \frac{(\lambda_{1-4})^{\varpi_3} \cdot (\lambda_{1-3})^{(j-\varpi_3)}}{j!\mu^j} \cdot P_0, \quad j = \varpi_3 + 1, \varpi_3 + 2, \ldots, \varpi_2. \tag{19}$$

For $\varpi_2 < j \leq \varpi_1$, local balance equations are

$$P_{\varpi_2+1} = \frac{\lambda_{1-2}}{(\varpi_2+1)\,\mu} \cdot P_{\varpi_2} = \frac{(\lambda_{1-4})^{\varpi_3} \cdot (\lambda_{1-3})^{(\varpi_2-\varpi_3)} \cdot \lambda_{1-2}}{(\varpi_2+1)! \cdot \mu^{(\varpi_2+1)}} \cdot P_0 \ldots$$

Therefore

$$P_j = \frac{(\lambda_{1-4})^{\varpi_3} \cdot (\lambda_{1-3})^{(\varpi_2-\varpi_3)} \cdot (\lambda_{1-2})^{(j-\varpi_2)}}{j!\mu^j} \cdot P_0, \quad j = \varpi_2 + 1, \varpi_2 + 2, \ldots, \varpi_1. \tag{20}$$

Finally, for $\varpi_1 < j \leq \varpi_T$, local balance equations are

$$P_{\varpi_1+1} = \frac{\lambda_1}{(\varpi_1+1)\,\mu} \cdot P_{\varpi_1} = \frac{(\lambda_{1-4})^{\varpi_3} \cdot (\lambda_{1-3})^{(\varpi_2-\varpi_3)} \cdot (\lambda_{1-2})^{(\varpi_1-\varpi_2)} \cdot \lambda_1}{(\varpi_1+1)! \cdot \mu^{(\varpi_1+1)}} \cdot P_0 \ldots$$

Therefore

$$P_j = \frac{(\lambda_{1-4})^{\varpi_3} \cdot (\lambda_{1-3})^{(\varpi_2-\varpi_3)} \cdot (\lambda_{1-2})^{(\varpi_1-\varpi_2)} \cdot (\lambda_1)^{(j-\varpi_1)}}{j! \cdot \mu^{(j)}} \cdot P_0, \quad j = \varpi_1 + 1, \ldots, \varpi_T. \tag{21}$$

P_0 is obtained from the normalizing equation

$$\sum_{j=0}^{\varpi_3} P_j + \sum_{j=\varpi_3+1}^{\varpi_2} P_j + \sum_{j=\varpi_2+1}^{\varpi_1} P_j + \sum_{j=\varpi_1+1}^{\varpi_T} P_j = 1.$$

Substituting and solving for P_0

$$P_0 = \left[\sum_{j=0}^{\varpi_3} \frac{\lambda_{1-4}^{j}}{j! \cdot \mu^j} + \sum_{j=\varpi_3+1}^{\varpi_2} \frac{\lambda_{1-4}^{\varpi_3} \cdot \lambda_{1-3}^{(j-\varpi_3)}}{j! \cdot \mu^j} + \sum_{j=\varpi_2+1}^{\varpi_1} \frac{\lambda_{1-4}^{\varpi_3} \cdot \lambda_{1-3}^{(\varpi_2-\varpi_3)} \cdot \lambda_{1-2}^{(j-\varpi_2)}}{j! \cdot \mu^j} + \sum_{j=\varpi_1+1}^{\varpi_T} \frac{\lambda_{1-4}^{\varpi_3} \cdot \lambda_{1-3}^{(\varpi_2-\varpi_3)} \cdot \lambda_{1-2}^{(\varpi_1-\varpi_2)} \cdot \lambda_{1}^{(j-\varpi_1)}}{j! \cdot \mu^j} \right]^{-1}. \quad (22)$$

ACKNOWLEDGMENT

The authors are thankful to the editors of this JSAC Special Issue and to the anonymous reviewers for their valuable suggestions, which improved the quality of the paper.

REFERENCES

[1] H. Holma and A. Toskala, *WCDMA for UMTS*. West Sussex, U.K.: Wiley, 2000.
[2] D. Hong and S. S. Rappaport, "Traffic model and performance analysis for cellular mobile radio telephone systems with prioritized and nonprioritized handoff procedures," *IEEE Trans. Veh. Technol.*, vol. VT-35, no. 3, pp. 77–92, Aug. 1986.
[3] C. H. Yoon and C. K. Un, "Performance of personal portable radio telephone systems with and without guard channels," *IEEE J. Sel. Areas Commun.*, vol. 11, no. 6, pp. 911–917, Aug. 1993.
[4] O. Yu and V. Leung, "Adaptive resource allocation for prioritized call admission over an ATM-based wireless PCN," *IEEE J. Sel. Areas Commun.*, vol. 15, no. 7, pp. 1208–1225, Sep. 1997.
[5] P. Ramanathan, K. M. Sivalingam, P. Agrawal, and S. Kishore, "Dynamic resource allocation schemes during handoff for mobile multimedia wireless networks," *IEEE J. Sel. Areas Commun.*, vol. 17, no. 7, pp. 1270–1283, Jul. 1999.
[6] O. Yu, "End-to-end dynamic adaptive QoS provisioning over GPRS wireless mobile network," *J. Mobile Netw. Appl.*, vol. 8, no. 3, pp. 255–267, 2003.
[7] S. Aissa *et al.*, "Call admission on the uplink and downlink of a CDMA system based on total received and transmitted powers," *IEEE Trans. Wireless Commun.*, vol. 3, no. 6, pp. 2407–2416, Nov. 2004.
[8] S. Shen *et al.*, "Intelligent call admission control for wideband CDMA cellular systems," *IEEE Trans. Wireless Commun.*, vol. 3, no. 5, pp. 1810–1821, Sep. 2004.
[9] F. A. Cruz-Perez and L. Ortigoza-Guerrero, "Flexible resource allocation strategies for class-based QoS provisioning in mobile networks," *IEEE Trans. Veh. Technol.*, vol. 53, no. 3, pp. 805–819, May 2004.
[10] C. Lindemann *et al.*, "Adaptive call admission control for QoS/revenue optimization in CDMA cellular networks," *J. Wireless Netw.*, vol. 10, no. 4, pp. 457–472, 2004.
[11] W. S. Jeon and D. G. Jeong, "Call admission control for CDMA mobile communications systems supporting multimedia services," *IEEE Trans. Wireless Commun.*, vol. 1, no. 4, pp. 649–659, Oct. 2002.
[12] B. Li *et al.*, "Call admission control for voice/data integrated cellular networks: Performance analysis and comparative study," *IEEE J. Sel. Areas Commun.*, vol. 22, no. 4, pp. 706–718, May 2004.
[13] H. Chen, S. Kumar, and C. C. J. Kuo, "Dynamic call admission control and resource reservation with interference guard margin (IGM) for CDMA systems," in *Proc. IEEE Wireless Commun. Netw. Conf.*, vol. 3, 2003, pp. 1568–1572.
[14] F. Hu and N. K. Sharma, "Priority-Determined multiclass handoff scheme with guaranteed mobile QoS in wireless multimedia networks," *IEEE Trans. Veh. Tech.*, vol. 53, no. 1, pp. 118–135, Jan. 2004.
[15] L. Huang, S. Kumar, and C. C. J. Kuo, "Adaptive resource allocation for multimedia QoS management in wireless networks," *IEEE Trans. Veh. Tech.*, vol. 53, no. 2, pp. 547–558, Mar. 2004.
[16] X. Chen, B. Li, and Y. Fang, "A dynamic multiple-threshold bandwidth reservation (DMTBR) scheme for QoS provisioning in multimedia wireless networks," *IEEE Trans. Wireless Commun.*, vol. 4, no. 2, pp. 583–592, Mar. 2005.
[17] O. Yu, E. Saric, and A. Li, "Adaptive prioritized admission over CDMA," in *Proc. IEEE Wireless Commun. Netw. Conf.*, vol. 2, Mar. 2005, pp. 1260–1265.
[18] O. Jennings and W. A. Massey, "A modified offered load approximation for nonstationary circuit switched networks," *J. Telecommun. Syst.*, vol. 7, pp. 229–251, 1997.
[19] L. Green and P. Kolesar, "The pointwise stationary approximation for queue with nonstationary arrivals," *Manage. Sci.*, vol. 37, pp. 84–97, 1991.
[20] W. A. Massey, "The analysis of queues with time-varying rates for telecommunication models," *J. Telecommun. Syst.*, vol. 21, no. 2, pp. 173–204, 2002.
[21] C. Knessl, "An exact solution for an $\mathrm{M(t)/M(t)/1}$ queue with time-dependent arrivals and service," *Queueing Syst.*, vol. 40, no. 3, pp. 233–245, 2002.
[22] OPNET Modeler [Online]. Available: www.opnet.com
[23] I. Katzela, *Modeling and Simulating Communication Networks: A Hands-On Approach Using OPNET*. Upper Saddle River, NJ: Prentice-Hall, 1998.
[24] T. Robertazzi, *Computer Networks and Systems: Queueing Theory and Performance Evaluation*. New York: Springer-Verlag, 2000.

Oliver Yu (S'80–M'89) received the B.A.Sc., M.A.Sc., and Ph.D. degrees in electrical and computer engineering from the University of British Columbia (UBC), Vancouver, BC, Canada, in 1981, 1991, and 1997, respectively.

From 1981 to 1985, he was a Member of Technical Staff at Microtel Pacific Research. From 1985 to 1986, he was an Engineering Manager at Soltech Industries. From 1986 to 1989, he was a team leader at Bell Northern Research (later renamed Nortel Networks). From 1992 to 1995, he was a Senior System Architect at Hughes Aircraft. From 1997 to 1999, he was a Section Manager at Motorola for GPRS wireless mobile network research and development. Since 1999, he has been an Assistant Professor in the Department of Electrical and Computer Engineering, University of Illinois at Chicago (UIC). His research interests are in the areas of 3G/4G wireless mobile networks, all-optical photonic networks, and next-generation Internet service provisioning.

Dr. Yu received the Career Award from the Department of Energy (DOE) in 2003.

Emir Saric (S'00) received the B.S. and M.S. degrees in electrical and computer engineering from the University of Illinois at Chicago (UIC) in 2001 and 2004, respectively. He is currently working towards the Ph.D. degree in electrical and computer engineering at UIC.

Since 2004, he has been a Research Assistant for Prof. O. Yu at the Networking and Wireless Communications Laboratory, UIC. His research interests include QoS provisioning (MAC and admission control) and performance evaluation of future cellular wireless networks and mobile ad hoc networks.

Anfei Li received the B.S. degree from the University of Science and Technology of China, Hefei, in 2002. He is currently working towards the Ph.D. degree in networking and wireless communication at the University of Illinois at Chicago (UIC).

His research interests include MAC protocols in 3G and 4G communication, wireless ad hoc and sensor networks, routing, and wavelength assignment in all optical networking.